



Identification of acetylshikonin as a novel tubulin polymerization inhibitor with antitumor activity in human hepatocellular carcinoma cells

Siming Hu¹, Yongchuan Li², Junqiu Zhou³, Kun Xu³, Yanqing Pang⁴, Ralf Weiskirchen⁵^, Matthias Ocker⁶^, Fen Ouyang³^

¹Department of Laboratory Medicine, Nanfang Hospital Taihe Branch, Guangzhou, China; ²First Clinical Medical College, Guangzhou University of Chinese Medicine, Guangzhou, China; ³Department of Laboratory Medicine, Nanfang Hospital Baiyun Branch, Southern Medical University, Guangzhou, China; ⁴Second Clinical Medical College, Guangzhou University of Chinese Medicine, Guangzhou, China; ⁵Institute of Molecular Pathobiochemistry, Experimental Gene Therapy, and Clinical Chemistry (IFMPEGKC), RWTH University Hospital Aachen, Aachen, Germany; ⁶Medical Department, Division of Hematology, Oncology, and Cancer Immunology Campus Charité Mitte, Charité University Medicine Berlin, Berlin, Germany

Contributions: (I) Conception and design: S Hu, F Ouyang; (II) Administrative support: Y Pang; (III) Provision of study materials or patients: Y Li; (IV) Collection and assembly of data: J Zhou; (V) Data analysis and interpretation: K Xu; (VI) Manuscript writing: All authors; (VII) Final approval of manuscript: All authors.

Correspondence to: Fen Ouyang, MD. Department of Laboratory Medicine, Nanfang Hospital Baiyun Branch, Southern Medical University, No. 1838, North Guangzhou Avenue, Baiyun District, Guangzhou 510420, China. Email: oyofficial@163.com.

Background: Microtubules are attractive targets for anticancer drugs. However, the microtubule-targeting agents (MTAs) currently in clinical use exhibit inevitable drug resistance. Therefore, there is an urgent need to discover novel MTAs for the clinical treatment of cancer.

Methods: Bioactive compounds extracted from *Lithospermum erythrorhizon* were assessed for *in vitro* anti-proliferative activities against a panel of human cancer cell lines using cell counting kit-8 (CCK-8) assay. Tubulin polymerization inhibition assay, colchicine competitive binding site assay, and immunofluorescence were used to validate the tubulin inhibition effect of acetylshikonin. Flow cytometry, Hoechst staining, and caspase-3 activity evaluation were performed to assess cell cycle arrest and cell apoptosis. 5,5',6,6'-tetrachloro-1,1',3,3'-tetramethylbenzimidazolylcarbocyanine iodide (JC-1) staining and dichlorodihydro-fluorescein diacetate (DCFH-DA) staining were used to evaluate mitochondrial membrane potential (MMP) and reactive oxygen species (ROS), respectively.

Results: Acetylshikonin exhibited potent anti-proliferative activities against a panel of human cancer cell lines (IC₅₀ values: 1.09–7.26 μM) and displayed comparable cytotoxicity against several drug-resistant cell lines. Further mechanism studies revealed that acetylshikonin induced cell cycle arrest of MHCC-97H cells at G₂/M phase, and significantly promoted apoptosis marked by a collapse of MMP and abnormal ROS accumulation.

Conclusions: In this study, acetylshikonin was identified as MTA against hepatocellular carcinoma and can serve as a promising lead compound for further development of anti-cancer drug, underscoring its potential clinical significance.

Keywords: Natural products (NPs); acetylshikonin; microtubule-targeting agent (MTA); anti-cancer

Submitted Oct 16, 2023. Accepted for publication Dec 08, 2023. Published online Dec 22, 2023.

doi: 10.21037/jgo-23-842

View this article at: <https://dx.doi.org/10.21037/jgo-23-842>

^ ORCID: Fen Ouyang, 0009-0003-5751-9970; Ralf Weiskirchen, 0000-0003-3888-0931; Matthias Ocker, 0000-0001-8263-6288.

Introduction

Natural products (NPs) have historically served as a valuable reservoir for drug discovery and have contributed significantly to the development of new treatment options for chemoprevention and cancer therapy (1,2). Numerous chemotherapeutic agents such as paclitaxel, vinblastine, and etoposide employed in cancer treatment today have either originated directly from natural sources or have been derived from NPs (3). The diverse bioactive compounds present in NPs provide a rich source for the discovery of novel anti-cancer agents (4).

Lithospermum erythrorhizon, a flowering plant in the Boraginaceae family, have been used for centuries in traditional Asian medicine, particularly in China, where is known as Zi Cao (5). Traditionally, the root extract of *Lithospermum erythrorhizon* has been used to treat dermatitis, burns, and wounds. Over the past three decades, the anti-inflammatory and anticancer effects have been extensively studied (6,7). Extracts from *Lithospermum erythrorhizon* have demonstrated promising anti-proliferative effects on various cancer cell lines (8). The main bioactive compounds in *Lithospermum erythrorhizon* responsible for its anti-cancer effects are naphthoquinone compounds, including shikonin, acetylshikonin, β,β -dimethylacrylshikonin, and shikonofuran (9,10). Studies on the potential anti-cancer mechanism of *Lithospermum erythrorhizon*, specifically its extracts or bioactive components, have mainly indicated the excessive activation of oxidative stress, disruption of mitochondrial function, cell cycle arrest and consequent induction of cell apoptosis (11,12). Meanwhile, the effects of *Lithospermum erythrorhizon* on the tubulin-microtubule

system have not been thoroughly studied.

Microtubules, composed of α - and β -tubulin protein subunits, are dynamic structures essential for various cellular processes including cell division, intracellular transportation, and cell shape maintenance (13). The dynamic nature and essential roles of the tubulin-microtubule system in cell division make them an attractive target for drugs aiming to disrupt cellular processes in rapidly dividing cancer cells (14,15). Microtubule-targeting agents (MTAs) can be broadly classified into 2 categories: (I) stabilizing agents, such as taxanes (e.g., paclitaxel and docetaxel), that promote microtubule assembly and inhibit disassembly (16); (II) destabilizing agents, including vinca alkaloids (e.g., vincristine and vinblastine), that inhibit microtubule assembly and promote disassembly (17). Mechanistic studies have elucidated that MTAs bind to specific sites on microtubules or tubulin subunits, affecting their polymerization and stability (18-20). By altering microtubule dynamics, MTAs disrupt the proper alignment and segregation of chromosomes during cell division, ultimately inhibiting cancer cell proliferation (21).

In this study, an initial screening was conducted of some reported bioactive compounds (Figure 1) extracted from *Lithospermum erythrorhizon* for their *in vitro* anti-proliferative activities against a panel of human cancer cell lines. Moreover, we first reported that acetylshikonin acted as an MTA to exert anti-cancer activity through conducting a tubulin polymerization inhibition assay, competitive binding assay, and intracellular immunofluorescence analyses. Further mechanism study showed that acetylshikonin disrupted the dynamic balance of the tubulin-microtubule system, interfered with the cell mitosis through inducing cell cycle arrest at G₂/M phase, and ultimately induced cell apoptosis via the intrinsic (mitochondrial) pathway. We present this article in accordance with the MDAR reporting checklist (available at <https://jgo.amegroups.com/article/view/10.21037/jgo-23-842/rc>).

Methods

Reagents

The chemical reagents used in our study including Acetylshikonin (lot number: A832580, 99% purity), Shikonin (lot number: S914687, 98% purity), Deoxyshikonin (lot number: D861265, 98% purity), β,β -dimethylacrylshikonin (lot number: D799242, 98% purity), Lithospermidin E, Shikonofuran A (lot number:

Highlight box

Key findings

- Acetylshikonin was first identified as a microtubule-targeting agent (MTA) against hepatocellular carcinoma.

What is known and what is new?

- Acetylshikonin was reported to possess a wide range of pharmacological activities, including anti-cancer, anti-inflammation, and anti-oxidation.
- Acetylshikonin was first evaluated for its interference effect on the tubulin-microtubule system.

What is the implication, and what should change now?

- The structure and potential effect as an MTA might provide a drug design strategy for anti-cancer drug development.

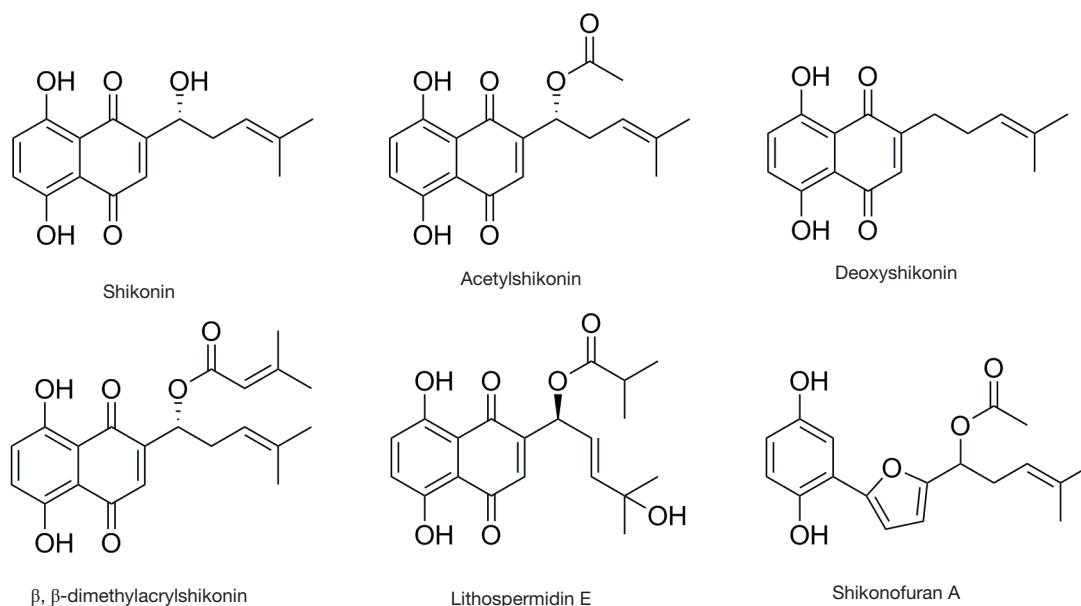


Figure 1 Chemical structures of the main bioactive compounds extracted from *Lithospermum erythrorhizon*.

C11637623, 99% purity) were all purchased from MACKLIN (Shanghai, China). Cell counting kit-8 (CCK-8) assay kit, DNA content assay kit (Solibao, Beijing, China) were obtained from Solibao (Beijing, China). Annexin V-FITC/PI double staining assay kit, caspase-3 enzyme activity kit, JC-1 kit were purchased from Beyotime (Shanghai, China). Other reagents were purchased from Sigma-Aldrich (St. Louis, MO, USA) unless otherwise specified.

Cell culture

The human cell lines used in this study were all commercially obtained from National Collection of Authenticated Cell Cultures (Shanghai, China). A549 [epithelial carcinoma lung cell line (22)], Caski [epidermoid cervical cancer cell line (23)], MHCC-97H [metastatic hepatocellular carcinoma cell line (24,25)], L-02 [a HeLa derivative, originally thought to originate from a normal fetal liver (26,27)], RWPE-1 [prostatic epithelial cell line (28)], and MCF-10A [breast epithelial cell line (29)] were cultivated in Dulbecco's modified Eagle medium (DMEM) containing 10% (v/v) heat-inactivated fetal bovine serum (FBS), 100 U/mL penicillin, and 100 mg/mL streptomycin. PC-3 [prostate carcinoma cell line (30)], HCT-8 [adenocarcinoma cell line (31)], MHCC-97H/

CDDP (cisplatin-resistant MHCC-97H cells), PC-3/ENZR (enzalutamide-resistant PC-3 cells), and HCT-8/VCR (vincristine-resistant HCT-8 cells) were cultivated in Roswell Park Memorial Institute (RPMI)-1640 medium containing 10% (v/v) heat-inactivated FBS, 100 U/mL penicillin, and 100 mg/mL streptomycin. Cells were cultured in a humidified incubator at 37 °C and 5% CO₂. The culture medium was replaced every 2–3 days. When the cell density reached more than 80%, cell passaging was performed.

Cell counting kit-8 (CCK-8) assay

CCK-8 is a widely used reagent for rapid and highly sensitive detection of cell proliferation and cytotoxicity. Briefly, 5×10^3 cells were seeded in 96-well plates for 24 hours. After sufficient cell adhesion, a series of compound concentrations (100 μL/well) were added and incubated for 48 hours. After 48 hours, 10 μL of CCK-8 solution (Beyotime, Shanghai, China) was added to each well. After 2 hours of incubation, the absorbance was measured at a wavelength of 450 nm. Cell toxicity was calculated based on the optical density (OD) values obtained from each group. The IC₅₀ values were obtained from 3 independent times experiment and the data were presented as the mean ± standard error of the mean (SEM).

In vitro tubulin polymerization assay

In vitro tubulin polymerization was performed following our previously reported method under the guidance of a commercial kit [cytoskeleton, cat.#BK011P; Cell Signaling Technology (CST), Danvers, MA, USA] (32). Briefly, purified tubulin (1 mg/mL) was dissolved in reaction buffer containing 80.0 mM piperazine-N,N'-bis(2-ethanesulfonic acid) sequei-sodium salt (pH 6.9), 0.5 mM ethylene glycol tetraacetic acid (EGTA), 2.0 mM MgCl₂, 1 mM GTP, and 10.2% glycerol. The solution was then incubated with or without compounds and warmed to 37 °C for 1 min. After addition of 55 µL of the tubulin reaction mix, the fluorescence intensity was monitored and recorded every 60 s over the period of 90 min at an excitation wavelength of 340 nm and an emission wavelength of 410 nm using multifunction microplate reader (Varioskan LUX; Thermo Fisher Scientific, Waltham, MA, USA).

Colchicine competitive binding assay

The colchicine competitive binding assay was performed according to our previously reported method (33). In 50 µL of G-PEM buffer, radioactive [³H]-labeled colchicine and 1% dimethyl sulfoxide (DMSO) were added. Then, each group was treated with indicated concentrations of target compounds and incubated with 1 µM tubulin for 1 hour. After column chromatography, the radioactivity of [³H]-labeled colchicine remaining in the solution was measured using a Perkin-Elmer analyzer (Perkin Elmer, Waltham, MA, USA), and non-linear regression analysis was performed using Origin 8.1 (OriginLab, Wellesley Hills, MA, USA). The radioactivity represented the content of colchicine in the solution, which indirectly reflected the competitive binding ability of the target compound with tubulin.

Immunofluorescence microscopy

MHCC-97H cells grown in logarithmic growth phase were seeded at a density of 30,000 cells/well and incubated overnight to allow the cells to adhere to the coverslips. After the supernatant was removed, fresh culture medium containing the test compounds was added and incubated for 24 hours. After incubation, the supernatant was discarded, and the cells were fixed with 4% paraformaldehyde for 30 min and followed by permeabilizing the cells with 0.5% Triton-X100 for 5 min. After that, the samples were blocked

with 5% bovine serum albumin (BSA) for 30 min and incubated with tubulin antibody (CST USA) overnight at 4 °C. Finally, the samples were incubated with goat anti-mouse IgG/Alexa-Fluor 488 antibody (Invitrogen, Waltham, MA, USA) for 1 hour and the nuclei of the cells were labelled with Hoechst 33342 (Sigma Aldrich, St. Louis, MO, USA) in the dark at room temperature for 15 min. After washing, the samples were immediately visualized on a Zeiss LSM 570 laser scanning confocal microscope (Carl Zeiss, Jena, Germany).

Ultrafiltration combined with liquid chromatography tandem mass spectrometry to investigate the binding mode of acetylshikonin with tubulin

The ultrafiltration method combined with liquid chromatography tandem mass spectrometry (LC-MS/MS) was used to investigate the binding mode of acetylshikonin according to our reported methods (34). Tubulin (3 mg/mL) was incubated with or without 30 mM colcemid or 30 mM acetylshikonin at 37 °C for 1 hour. Then, the incubation mixture was subjected to ultrafiltration centrifugation, and the solution upper membrane and the filtrate were separately collected to quantify the concentration of tested compounds using LC-MS/MS. The group which contained colcemid or acetylshikonin was used as the control group.

Flow cytometry analysis of cell cycle

MHCC-97H cells reached the logarithmic growth phase were collected and seeded into 6-well plates at a density of 20,000 cells/well. The plates were then incubated overnight to allow cell adhesion. Next, the cells were treated with 0.75, 1.5, and 3.0 µM acetylshikonin for 48 hours. After treatment, the collected cells were treated with pre-cooled 75% ethanol for overnight fixation at -20 °C. After centrifugation, the fixed solution was washed away with phosphate-buffered saline (PBS). Following the instructions of the DNA content assay kit (Solibao, Beijing, China), each sample was treated with 100 µL RNase at 37 °C for 30 minutes to remove RNA interference. Then, 400 µL propidium iodide (PI) solution was added in the dark for 15 min. A total of 10,000 events were measured by flow cytometry (Epics XL; Beckman Coulter, Brea, CA, USA) at 488 nm. The data regarding the number of cells in different phases of the cell cycle was analyzed by EXPO32 ADC analysis software (Beckman Coulter).

Annexin V-FITC/PI double staining assay

The cells samples were treated and collected as described in the cell cycle analysis. For apoptosis analysis, the collected samples were performed under the guidance of Annexin-V-FITC/PI kit (Beyotime, China). After incubation with 5 μ L of Annexin-V-FITC buffer at room temperature for 15 min, PI solution was then added drop-wise and incubated for 10 min. Almost 10,000 events were collected for flow cytometry analysis (Epics XL). The percentage of apoptotic cells was calculated using EXPO32 ADC analysis software.

Caspase-3 activity

A Caspase-3 Activity Assay Kit was used to detect caspase-3 enzyme activity in cells using colorimetric method according to the manufacturer's instructions (Beyotime, China). Briefly, the cells were seeded and treated as described in the cell cycle analysis. Then, the cells were treated with 5 μ M GreenNuc™ Caspase-3 Substrate and incubated in dark at 37 °C for 30 minutes. The caspase-3 activity was monitored by the fluorescence intensity at an excitation wavelength of 485 nm and an emission wavelength of 515 nm using a microplate reader (Varioskan LUX).

Intracellular mitochondrial membrane potential (MMP) detection

The cell samples were treated and collected as described in the cell cycle analysis. The collected cells were resuspended in 0.5 mL of cell culture medium and then 0.5 ml of 5,5',6,6'-tetrachloro-1,1',3,3'-tetramethylbenzimidazolyl carbocyanine iodide (JC-1) working solution (Beyotime, China) was added. The mixture was incubated at 37 °C for 20 min. After incubation, the cells were centrifuged at 600 \times g for 3–4 min at 4 °C, and the cell pellet was washed twice with JC-1 staining buffer (1 \times). The MMP was observed using a fluorescence microscope and analyzed using a flow cytometer.

Intracellular reactive oxygen species (ROS) detection

The cell samples were treated and collected as described in the cell cycle analysis. The collected cells were incubated with 10 μ M dichloro-dihydro-fluorescein diacetate (DCFH-DA; Sigma Aldrich, USA) at 37 °C for 30 min. After incubation, the cells were centrifuged at 600 \times g for 3–4 min

at 4 °C, and washed twice with PBS. The intracellular ROS was observed using a fluorescence microscope and analyzed using a flow cytometer.

Statistical analysis

SEM from at least three independent experiments were obtained and presented. Unless otherwise indicated, the differences were considered to be statistically significant at $P < 0.05$, $P < 0.001$ followed by Student's unpaired *t*-test for two-group comparison using one-way analysis of variance (ANOVA). GraphPad Prism Software version 8.0 (GraphPad Inc., La Jolla, CA, USA) was used for statistical analysis.

Results

In vitro anti-proliferative activity evaluation

For the initial screening, some commercially bioactive compounds extracted from *Lithospermum erythrorhizon* were selected to evaluate their *in vitro* anti-proliferative activities against a panel of human cancer cell lines. As summarized in *Table 1*, all of these bioactive compounds (*Figure 1*) extracted from *Lithospermum erythrorhizon* displayed anti-proliferative activities against several human cancer cell lines, including human non-small cell lung cancer cell line (A549), human epithelial cervical carcinoma cell line (Caski), human liver carcinoma cell line (MHCC-97H), human prostatic cancer cell line (PC-3), and human colorectal carcinoma cell line (HCT-8). Among them, acetylshikonin displayed the best anti-proliferative activities with an IC₅₀ below 10 μ M. Hence, acetylshikonin was selected as the optimized compound for further study.

Selectivity of acetylshikonin towards normal cells and cancer cells

One of the factors limiting the development of anticancer drugs is potential toxicity towards normal cells. Therefore, the selectivity of acetylshikonin towards both normal cells and cancer cells was also evaluated. As shown in *Table 2*, acetylshikonin exhibited relatively low cytotoxicity towards L-02 and RWPE-1 cell lines, with selectivity ratios of 9.41- and 2.49-fold, respectively. Additionally, acetylshikonin displayed nearly equivalent anti-proliferative activity against both breast cancer cells and normal breast cells.

Table 1 Anti-proliferative activities of several bioactive compounds extracted from *Lithospermum erythrorhizon*

Compounds	IC ₅₀ (μM), mean ± SE				
	A549	Caski	MHCC-97H	PC-3	HCT-8
Acetylshikonin	3.12±0.22	2.93±0.47	1.09±0.27	3.52±0.36	7.26±0.14
Shikonin	10.63±0.45	3.98±0.11	5.98±0.18	19.11±0.15	15.24±0.55
Deoxyshikonin	3.48±0.19	6.16±0.12	7.54±0.021	25.72±0.33	19.25±0.44
β,β-dimethylacrylshikonin	12.69±0.17	22.77±0.83	36.69±0.23	18.76±0.32	52.69±1.36
Lithospermidin E	12.02±0.28	9.66±0.89	5.56±0.85	32.21±1.17	20.72±0.35
Shikonofuran A	72.22±4.24	18.86±1.39	9.56±0.15	18.89±2.21	58.72±3.21

IC₅₀, half-maximal drug inhibitory concentration; SE, standard error.

Table 2 Selectivity of Acetylshikonin towards normal cells and cancer cells

Cell lines	IC ₅₀ (μM), mean ± SE	Selectivity ratio
MHCC-97H	1.09±0.27	9.41
L-02	10.26±0.24	–
PC-3	3.52±0.36	2.49
RWPE-1	8.75±0.18	–
MCF-7	7.15±0.11	1.05
MCF-10A	7.66±0.56	–

Selectivity ratio = (IC₅₀ of human normal cells)/(IC₅₀ of corresponding cancer cell lines). IC₅₀, half-maximal drug inhibitory concentration; SE, standard error.

Table 3 Cytotoxicity of acetylshikonin towards drug-resistant cancer cell lines

Cell lines	IC ₅₀ (μM), mean ± SE	Resistance index
MHCC-97H	1.09±0.27	0.78
MHCC-97H/CDDP	0.85±0.01	–
PC-3	3.52±0.36	1.20
PC-3/ENZR	4.22±0.17	–
HCT-8	7.26±0.14	0.90
HCT-8/VCR	6.51±0.62	–

Resistance index = (IC₅₀ of drug-resistance cell lines)/(IC₅₀ of corresponding cancer cell lines). MHCC-97H/CDDP, MHCC-97H cell line resistant to cisplatin; PC-3/ENZR, PC-3 cell line resistant to enzalutamide; HCT-8/VCR, HCT-8 cell line resistant to vincristine.

Cytotoxicity of acetylshikonin towards drug-resistant cancer cell lines

In addition to drug safety, multi-drug resistance is another factor limiting the development of anticancer drugs. In order to evaluate the cytotoxicity of acetylshikonin towards drug-resistant cancer cell lines, several commercially available

drug-resistant cell lines including cisplatin-resistant cell line MHCC-97H/CDDP, enzalutamide-resistant cell line PC-3/ENZR, and vincristine-resistant cell lines HCT-8/VCR were evaluated. As shown by the results summarized in *Table 3*, acetylshikonin displayed nearly or even better activity towards drug-resistance cancer cell lines.

Tubulin polymerization inhibition activity of acetylshikonin

MTAs interfere with microtubule dynamics and disrupt their normal functions, leading to eventual cell death. In this study, we also evaluated the tubulin polymerization inhibition activity of acetylshikonin. Firstly, our research aimed to determine the effect of acetylshikonin on the tubulin–microtubule system, specifically whether it acts as a microtubule stabilizer or a microtubule depolymerizer. As presented in *Figure 2A*, the enhancement of fluorescence intensity was inhibited by colchicine, a well-known microtubule depolymerizer, and was promoted by taxol, a well-known microtubule stabilizer. Similarly to colchicine, acetylshikonin can be classified as a microtubule depolymerizer based on its observed ability to inhibit tubulin polymerization. Then, as shown in *Figure 2B*, a series of treated concentrations of acetylshikonin were incubated with tubulin to obtain the IC₅₀ value that inhibited tubulin polymerization (5.98±0.02 μM). To visualize the interference of acetylshikonin on the intracellular tubulin–microtubule system, the immunofluorescence analysis was applied. As illustrated in *Figure 2C*, in the group of untreated cells, the microtubules exhibited an organized and filamentous arrangement surrounding the cell nucleus. However, upon treatment with acetylshikonin, the normal morphology of microtubules was significantly disrupted, characterized by the disappearance of filamentous structures, shrinkage, and even punctate distribution.

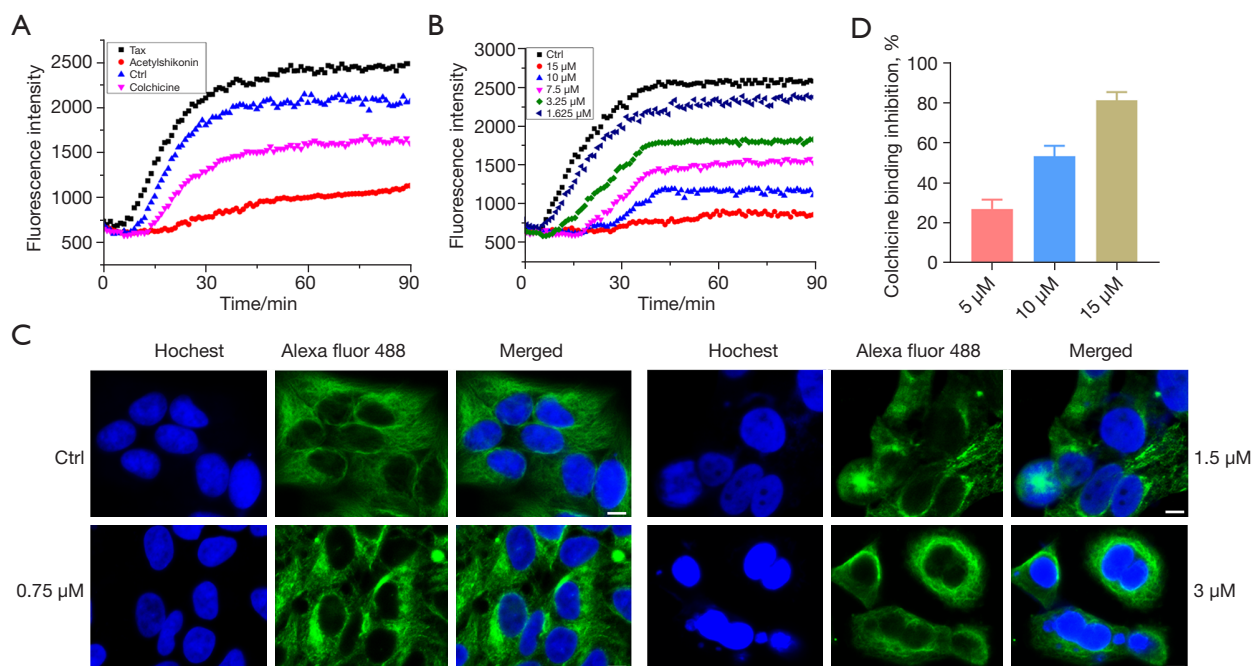


Figure 2 Acetylshikonin inhibited tubulin polymerization. (A,B) *In vitro* tubulin polymerization inhibition activity evaluation of compound taxol (10 μ M), colchicine (10 μ M), acetylshikonin (5 μ M) (A) and indicated concentrations of acetylshikonin (B). Purified tubulin was incubated in the absence (control) or presence of compounds at the indicated concentrations. The fluorescence intensity was monitored in emission at 410 nm over a 90 min period at 37 $^{\circ}$ C (excitation wavelength of 340 nm). (C) The immunofluorescence images of intracellular microtubule were detected with an LSM 570 laser confocal microscope (Carl Zeiss, Jena, Germany) in the absence (control) or presence of acetylshikonin at the indicated concentrations. (D) Competitive combining capacity of acetylshikonin in the tubulin-microtubule system, which was detected by a colchicine competition binding assay. The experiments were performed at least 3 independent times, and representative images are shown. Scale bars are 10 μ m.

Furthermore, this phenomenon became more pronounced with increasing concentrations of acetylshikonin. Finally, we also investigated the binding mode of acetylshikonin with tubulin. The results of colchicine competitive binding assay (Figure 2D) showed that acetylshikonin inhibited tubulin polymerization through binding with colchicine in a dose-dependent manner.

Acetylshikonin binds irreversibly to tubulin

Based on the aforementioned results demonstrating that acetylshikonin binds to tubulin at the colchicine binding site, our subsequent investigation aimed to determine whether this binding mode was irreversible. As shown in Figure 3A,3B, colcemid (a reported reversible tubulin inhibitor) and acetylshikonin were incubated with tubulin protein, respectively, followed by ultrafiltration. In the acetylshikonin-treated group, the filtrate showed almost no

detectable peak of acetylshikonin, whereas in the colcemid-treated group, approximately 67.8% of colcemid was detected in the filtrate. These results demonstrated that the binding mode of colcemid with tubulin was disrupted by the ultrafiltration method, indicating that this binding mode of colcemid is indeed reversible. In contrast, the binding mode of acetylshikonin was irreversible. The immunofluorescence images in Figure 3C also confirmed the same results. When the cells had been treated with colcemid or acetylshikonin for 8 hours, the obvious morphological alteration of intracellular microtubule was observed and this disruption effect was significantly restored upon removal of colcemid. Meanwhile, even after removing acetylshikonin, the microtubule morphology did not recover. Instead, with prolonged treatment time, the microtubules became more contracted and clustered around the cell nucleus. Altogether, these results demonstrated that acetylshikonin binds to tubulin in an irreversible way.

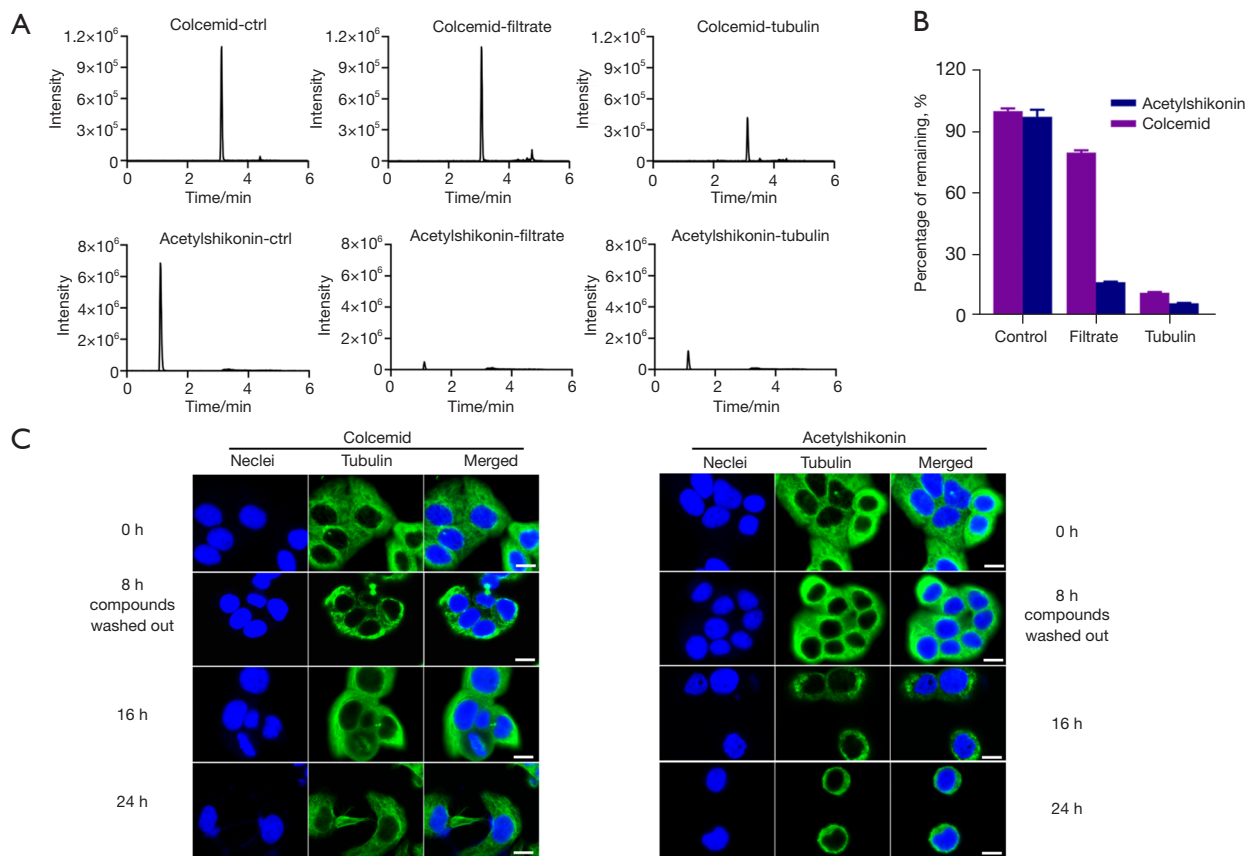


Figure 3 Acetylshikonin binds irreversibly to tubulin. (A) Quantification of residual compounds using LC-MS/MS. Tubulin (3 mg/mL) incubated with 30 μ M colcemid or 30 μ M acetylshikonin at 37 $^{\circ}$ C for 1 h. Then, the incubation mixture was subjected to ultrafiltration centrifugation, and the solution upper membrane and the filtrate were separately collected to quantify the concentration of tested compounds using LC-MS/MS. (B) The percentages of remaining compounds in each part. (C) The immunofluorescence images of intracellular microtubules. MHCC-97H cells were treated with high concentrations of colcemid (10 μ M) or acetylshikonin (10 μ M) for 8 h, then the compounds were removed and further cultured to 24 h. At 0-, 8-, 16-, and 24-h points, microtubule morphology was detected by an LSM 570 laser confocal microscope (Carl Zeiss). Scale bar = 5 μ m. The representative images of at least 3 independent experiments were shown. LC-MS/MS, liquid chromatography tandem mass spectrometry.

Acetylshikonin arrested cell cycle at G_2/M phase

Microtubules play a critical role in regulating the cell cycle. During cell division, microtubules form the mitotic spindle, which is responsible for segregating the chromosomes into daughter cells. The dynamic assembly and disassembly of microtubules drives various stages of the cell cycle, including mitosis and cytokinesis. Hence, considering the vital role of microtubule in the cell cycle, we used flow cytometry to evaluate the arrest effect of acetylshikonin on cell cycle. As presented in Figure 4, after MHCC-97H cells were treated with acetylshikonin for 24 hours, the cell cycle was significantly arrested at the G_2/M phase.

Acetylshikonin-induced cell apoptosis

It has been reported that MTAs disrupt the normal dynamic equilibrium of tubulin–microtubule system, arrest cell cycle, and eventually induce cell apoptosis. In this study, we also evaluated the apoptosis-inducing effect of acetylshikonin in MHCC-97H cell line. As illustrated in Figure 5A, an obvious apoptotic body was observed in the acetylshikonin-treated group, and as the treated concentrations increased, particularly in the high-dose compound treatment group (3 μ M), the typical features of apoptotic including significant reduction in nuclear volume, chromatin condensation, and nuclear fragmentation were observed.

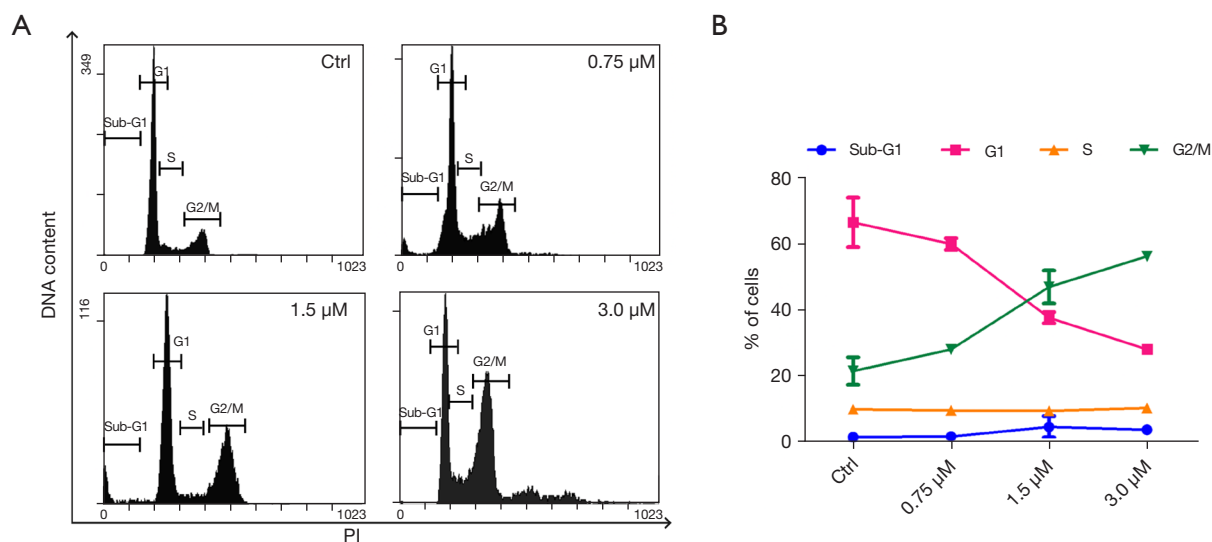


Figure 4 The cell cycle arrest effect of acetylshikonin. (A) MHCC-97H cells were exposed with or without acetylshikonin at the indicated concentrations for 24 hours and then harvested and stained with PI solution for flow cytometry analysis. The experiment was repeated for 3 independent times, and a representative experiment is presented. (B) The percentage of cells in each cell cycle phase was quantitatively analyzed using EXPO32 ADC analysis software. PI, propidium iodide.

The apoptosis-inducing effect of acetylshikonin was also evidenced by Annexin V-FITC/PI double staining assay and the activation of caspase-3. As shown in *Figure 5B, 5C*, as the treated-concentration of acetylshikonin gradually increased, there was a progressive increase in the proportion of cells undergoing early and late-stage apoptosis. Moreover, the caspase-3 activity in the acetylshikonin-treated group was significantly increased through the GreenNuc™ Caspase-3 Assay Kit (*Figure 5D*).

Cell apoptosis is closely associated with mitochondrial dysfunction and oxidative damage, typically embodied by a decrease in MMP and accumulation of ROS. Based on the results obtained above, acetylshikonin could induce apoptosis in MHCC-97H cells. Therefore, it is reasonable to speculate that it may also affect the mitochondrial function and oxidative stress system. The cell-permeable fluorogenic probe DCFH-DA and JC-1 were used to detect the intracellular ROS level and MMP, respectively. As shown in *Figure 6A-6C*, acetylshikonin significantly induced ROS accumulation in a dose-dependent manner, characterized by the enhanced fluorescence intensity. Decreased MMP has been implicated as an early event in apoptotic cells. The relative ratio of red to green fluorescence can be used to measure the extent of mitochondrial depolarization, thus can be used as an early indicator of cell apoptosis. As presented in *Figure 6D-6F*,

in the control group, the MMP was relatively high, and JC-1 aggregated in the mitochondrial matrix, forming J-aggregates that emitted red fluorescence. However, with the treated concentrations of acetylshikonin being increased, the MMP decreased, preventing the aggregation of JC-1 in the mitochondrial matrix and existing as monomers that emit green fluorescence, which indicated that mitochondrial depolarization happened and acetylshikonin could induce cell apoptosis.

Discussion

NPs are of great importance in drug discovery and biological research (1). *Lithospermum erythrorhizon*, a flowering plant in the Boraginaceae family which is known as Zi Cao in China was reported to possess a wide range of pharmacological activities (5-7). In our study, some bioactive compounds extracted from *Lithospermum erythrorhizon* were selected to evaluate their *in vitro* anti-proliferative activity against a panel of human cancer cell lines. Among them, acetylshikonin displayed the best anti-proliferative activities with IC_{50} below 10 μ M (*Table 1*). Why these compounds with extremely similar structures exhibit differences in anti-tumor activity is the subject that we will investigate in further study. Meanwhile, acetylshikonin will be used as the lead compound for our follow-up anti-cancer drug design.

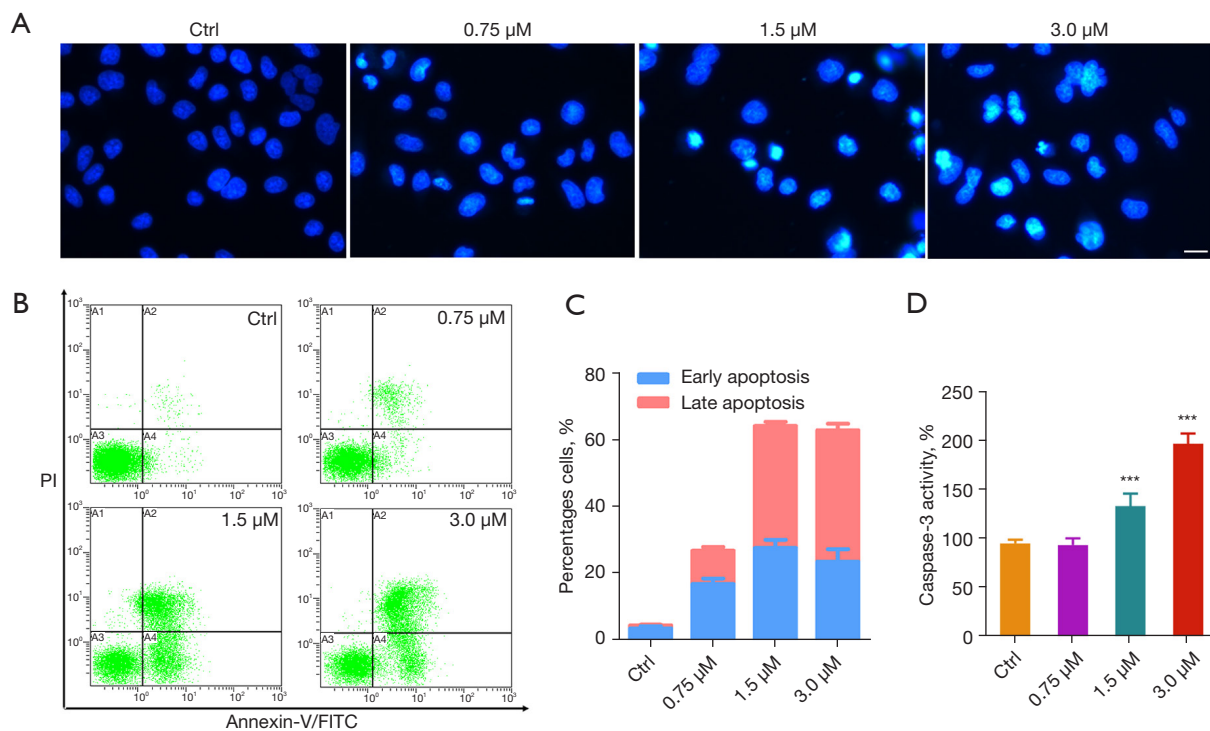


Figure 5 Acetylshikonin induced cell apoptosis. (A) The Hoechst 33342 staining of MHCC-97H cells treated with or without acetylshikonin at indicated concentrations; Scale bar: 10 μm . (B,C) Flow cytometry analysis of MHCC-97H cells stained with the Annexin V/FITC-PI double staining solution. (D) Caspase-3 activity was evaluated using a GreenNuc™ caspase-3 assay kit through a multifunctional microplate reader (Molecular Devices, Flex Station 3). The excitation and emission wavelength was set as 485 and 515 nm, respectively. All data were obtained from three independent experiments and the representative images were shown. Data were presented as the mean \pm SEM. ***, $P < 0.001$, significantly different compared to the control group by t -test. SEM, standard error of the mean.

Interestingly, acetylshikonin displayed selectivity for several human cancer cell lines and normal cell lines (Table 2). Except for the safety evaluation in the cell-based assay, the *in vivo* acute toxicity evaluation of acetylshikonin will be performed in the further study. Moreover, acetylshikonin displayed nearly or even better activity towards drug-resistance cancer cell lines (Table 3). The causes of anti-cancer drug resistance are multifactorial. Several key factors contribute to the development of drug resistance in tumors include genetic alterations, such as mutations or amplifications of drug targets, activation of cellular survival pathways, enhanced DNA repair mechanisms, and the overexpression of efflux pump named P-glycoprotein (P-gp). Additionally, tumor heterogeneity, tumor microenvironment factors, and the adaptive response of tumor cells to treatment can also play a role in the development of drug resistance (14). Overall, the underlying mechanisms of tumor drug resistance are complex and can vary depending on the specific tumor type and treatment regimen. The

specific molecular mechanisms underlying drug resistance will be investigated in detail in our further research.

In this study, acetylshikonin was first validated as an MTA through irreversible binding with colchicine site (Figures 2,3). However, the specific amino acid residues involved in tubulin have not yet been identified, which might be elucidated through LC-MS/MS method.

In the mechanism study, acetylshikonin was shown to induce cell cycle arrest at the G_2/M phase (Figure 4). As is commonly known, cell cycle progression relies on the activation of cyclin-dependent kinases (CDKs), which associate with cyclins to regulate different phases of the cell cycle. In particular, the cyclin B and Cdc2 kinase complex plays a crucial role in initiating the M phase. Phosphorylation of Cdc2 is known to activate its phosphatase activity, which is necessary for the activation of the Cdc2/cyclin B1 complex and the entry into mitosis (16). To understand the specific mechanisms underlying the cell cycle arrest induced by acetylshikonin, it is important to investigate its impact on

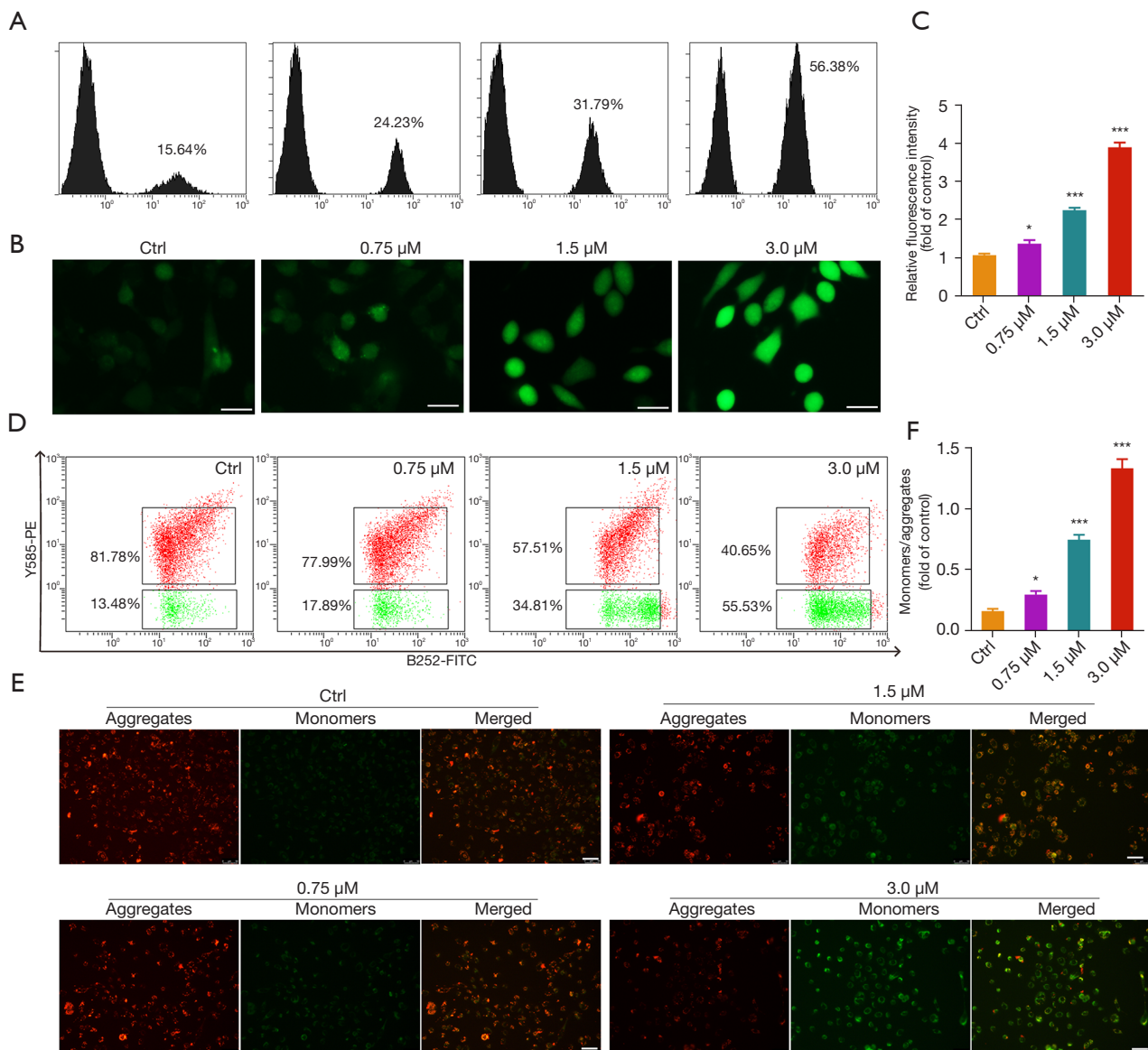


Figure 6 Acetylshikonin induced ROS accumulation and MMP decreased. MHCC-97H cells were treated with the indicated concentrations of acetylshikonin for 24 h. (A-C) The harvested cells were incubated with 10 μ M DCFH-DA at 37 $^{\circ}$ C for 30 min and ROS was quantified by flow cytometry (EXPO32 ADC), and intracellular ROS were acquired using fluorescence microscope (Life Technologies, EVOS FL Auto, USA). (D-F) Intracellular MMP was detected by JC-1 solution at 37 $^{\circ}$ C for 30 min and then monitored by fluorescence microscopy and flow cytometry. Representative images from three independent experiments are shown. Scale bar: 10 μ m. ROS, reactive oxygen species; MMP, mitochondrial membrane potential; DCFH-DA, dichloro-dihydro-fluorescein diacetate; JC-1, 5,5',6,6'-tetrachloro-1,1',3,3'-tetramethylbenzimidazolylcarbocyanine iodide.

the targeted cyclins or specific signaling pathways involved in cell cycle regulation. Further exploration of these aspects will provide valuable insights into the precise molecular mechanisms through which acetylshikonin exerts its arrest effect on cell cycle progression.

Finally, acetylshikonin was validated to induce cell apoptosis through the decrease of caspase 3 activity, ROS abnormal accumulation, and mitochondrial depolarization (Figures 5,6). As we all know, except for the classical caspase-dependent apoptosis signaling pathway, membrane death

receptor-mediated apoptosis and endoplasmic reticulum stress-mediated apoptosis are other important signaling pathways (27). Additional investigations were conducted to reveal whether acetylshikonin is involved in other apoptotic signaling pathways.

Conclusions

In this study, we have firstly validated that the NP acetylshikonin exerts potent anti-proliferative activity through targeting tubulin-microtubule system. Acetylshikonin acts as a microtubule depolymerizer by inhibiting tubulin polymerization at the colchicine-binding site. Additionally, acetylshikonin arrested cell cycle at the G₂/M phase, induced ROS accumulation and MMP collapse, and ultimately led to cell apoptosis. Therefore, the anticancer activity of acetylshikonin deserves further investigation for cancer therapy.

Acknowledgments

Funding: This research was funded by President Foundation of Baiyun Branch of Nanfang Hospital (No. BYYZ23008), Science and Technology Planning Project of Guangzhou (No. 202201020349), Department of Education Characteristic Innovation Project of Colleges and Universities of Guangdong Province (No. 2021KTSCX023), and the Scientific Research Project of Guangdong Province of Traditional Chinese Medicine (No. 20221164).

Footnote

Reporting Checklist: The authors have completed the MDAR reporting checklist. Available at <https://jgo.amegroups.com/article/view/10.21037/jgo-23-842/rc>

Data Sharing Statement: Available at <https://jgo.amegroups.com/article/view/10.21037/jgo-23-842/dss>

Peer Review File: Available at <https://jgo.amegroups.com/article/view/10.21037/jgo-23-842/prf>

Conflicts of Interest: All authors have completed the ICMJE uniform disclosure form (available at <https://jgo.amegroups.com/article/view/10.21037/jgo-23-842/coif>). The authors have no conflicts of interest to declare.

Ethical Statement: The authors are accountable for all aspects of the work in ensuring that questions related

to the accuracy or integrity of any part of the work are appropriately investigated and resolved.

Open Access Statement: This is an Open Access article distributed in accordance with the Creative Commons Attribution-NonCommercial-NoDerivs 4.0 International License (CC BY-NC-ND 4.0), which permits the non-commercial replication and distribution of the article with the strict proviso that no changes or edits are made and the original work is properly cited (including links to both the formal publication through the relevant DOI and the license). See: <https://creativecommons.org/licenses/by-nc-nd/4.0/>.

References

1. Atanasov AG, Zotchev SB, Dirsch VM, et al. Natural products in drug discovery: advances and opportunities. *Nat Rev Drug Discov* 2021;20:200-16.
2. Ebenezer O, Shapi M, Tuszynski JA. A Review of the Recent Developments of Molecular Hybrids Targeting Tubulin Polymerization. *Int J Mol Sci* 2022;23:4001.
3. Chopra B, Dhingra AK. Natural products: A lead for drug discovery and development. *Phytother Res* 2021;35:4660-702.
4. Prieto JM, Hanafi MMM. Advances in Molecular Regulation of Prostate Cancer Cells by Top Natural Products of Malaysia. *Curr Issues Mol Biol* 2023;45:1536-67.
5. Guo C, He J, Song X, et al. Pharmacological properties and derivatives of shikonin-A review in recent years. *Pharmacol Res* 2019;149:104463.
6. Wang J, Liu L, Sun XY, et al. Evidence and Potential Mechanism of Action of Lithospermum erythrorhizon and Its Active Components for Psoriasis. *Front Pharmacol* 2022;13:781850.
7. Choi YH, Kim GS, Choi JH, et al. Ethanol extract of Lithospermum erythrorhizon Sieb. et Zucc. promotes osteoblastogenesis through the regulation of Runx2 and Osterix. *Int J Mol Med* 2016;38:610-8.
8. Rajasekar S, Park DJ, Park C, et al. In vitro and in vivo anticancer effects of Lithospermum erythrorhizon extract on B16F10 murine melanoma. *J Ethnopharmacol* 2012;144:335-45.
9. Liao M, Yan P, Liu X, et al. Spectrum-effect relationship for anti-tumor activity of shikonins and shikonofurans in medicinal Zicao by UHPLC-MS/MS and chemometric approaches. *J Chromatogr B Analyt Technol Biomed Life Sci* 2020;1136:121924.
10. Hu Y, Jiang Z, Leung KS, et al. Simultaneous determination of naphthoquinone derivatives in

- Boraginaceous herbs by high-performance liquid chromatography. *Anal Chim Acta* 2006;577:26-31.
11. Olatunde OZ, Yong J, Lu C, et al. A Review on Shikonin and Its Derivatives as Potent Anticancer Agents Targeted against Topoisomerases. *Curr Med Chem* 2023. [Epub ahead of print]. doi: 10.2174/0929867330666230208094828.
 12. Zhang Z, Bai J, Zeng Y, et al. Pharmacology, toxicity and pharmacokinetics of acetylshikonin: a review. *Pharm Biol* 2020;58:950-8.
 13. Cassimeris L, Skibbens RV. Regulated assembly of the mitotic spindle: a perspective from two ends. *Curr Issues Mol Biol* 2003;5:99-112.
 14. Tangutur AD, Kumar D, Krishna KV, et al. Microtubule Targeting Agents as Cancer Chemotherapeutics: An Overview of Molecular Hybrids as Stabilizing and Destabilizing Agents. *Curr Top Med Chem* 2017;17:2523-37.
 15. Fong A, Durkin A, Lee H. The Potential of Combining Tubulin-Targeting Anticancer Therapeutics and Immune Therapy. *Int J Mol Sci* 2019;20:586.
 16. Christensen SB. Drugs That Changed Society: Microtubule-Targeting Agents Belonging to Taxanoids, Macrolides and Non-Ribosomal Peptides. *Molecules* 2022;27:5648.
 17. de la Roche NM, Mühlethaler T, Di Martino RMC, et al. Novel fragment-derived colchicine-site binders as microtubule-destabilizing agents. *Eur J Med Chem* 2022;241:114614.
 18. Zhou X, Fu YH, Zou YY, et al. Discovery of Simple Diacylhydrazine-Functionalized Cinnamic Acid Derivatives as Potential Microtubule Stabilizers. *Int J Mol Sci* 2022;23:12365.
 19. Yan J, Zhuang Q, Li Z, et al. MIL-1, a novel antitumor agent derived from natural product millepachine, acts as tubulin polymerization inhibitor for the treatment of hepatocellular carcinoma. *Eur J Pharmacol* 2021;898:173975.
 20. Pang Y, Lin H, Ou C, et al. Design, synthesis, and biological evaluation of novel benzodiazepine derivatives as anticancer agents through inhibition of tubulin polymerization in vitro and in vivo. *Eur J Med Chem* 2019;182:111670.
 21. Han HJ, Park C, Hwang J, et al. CPPF, A Novel Microtubule Targeting Anticancer Agent, Inhibits the Growth of a Wide Variety of Cancers. *Int J Mol Sci* 2020;21:4800.
 22. Giard DJ, Aaronson SA, Todaro GJ, et al. In vitro cultivation of human tumors: establishment of cell lines derived from a series of solid tumors. *J Natl Cancer Inst* 1973;51:1417-23.
 23. Pattillo RA, Hussa RO, Story MT, et al. Tumor antigen and human chorionic gonadotropin in CaSki cells: a new epidermoid cervical cancer cell line. *Science* 1977;196:1456-8.
 24. Li Y, Tang ZY, Ye SL, et al. Establishment of cell clones with different metastatic potential from the metastatic hepatocellular carcinoma cell line MHCC97. *World J Gastroenterol* 2001;7:630-6.
 25. Zhang L, Yuan L, Li D, et al. Identification of potential prognostic biomarkers for hepatocellular carcinoma. *J Gastrointest Oncol* 2022;13:812-21.
 26. Weiskirchen R. Letter to the Editor: LO2, a misidentified cell line: Some data should be interpreted with caution. *Hepatology* 2023;77:E66.
 27. Weiskirchen R. Research reporting guidelines for cell lines: more than just a recommendation. *Ann Transl Med* 2023. [Epub ahead of print]. doi: 10.21037/atm-23-1208.
 28. Webber MM, Bello D, Quader S. Immortalized and tumorigenic adult human prostatic epithelial cell lines: characteristics and applications. Part I. Cell markers and immortalized nontumorigenic cell lines. *Prostate* 1996;29:386-94.
 29. Soule HD, Maloney TM, Wolman SR, et al. Isolation and characterization of a spontaneously immortalized human breast epithelial cell line, MCF-10. *Cancer Res* 1990;50:6075-86.
 30. Kaighn ME, Lechner JF, Narayan KS, et al. Prostate carcinoma: tissue culture cell lines. *Natl Cancer Inst Monogr* 1978;(49):17-21.
 31. Tompkins WA, Watrach AM, Schmale JD, et al. Cultural and antigenic properties of newly established cell strains derived from adenocarcinomas of the human colon and rectum. *J Natl Cancer Inst* 1974;52:1101-10.
 32. Zhou J, Pang Y, Zhang W, et al. Discovery of a Novel Stilbene Derivative as a Microtubule Targeting Agent Capable of Inducing Cell Ferroptosis. *J Med Chem* 2022;65:4687-708.
 33. Yan J, Pang Y, Sheng J, et al. A novel synthetic compound exerts effective anti-tumour activity in vivo via the inhibition of tubulin polymerisation in A549 cells. *Biochem Pharmacol* 2015;97:51-61.
 34. Yan J, Xu Y, Jin X, et al. Structure modification and biological evaluation of indole-chalcone derivatives as anti-tumor agents through dual targeting tubulin and TrxR. *Eur J Med Chem* 2022;227:113897.

Cite this article as: Hu S, Li Y, Zhou J, Xu K, Pang Y, Weiskirchen R, Ocker M, Ouyang F. Identification of acetylshikonin as a novel tubulin polymerization inhibitor with antitumor activity in human hepatocellular carcinoma cells. *J Gastrointest Oncol* 2023;14(6):2574-2586. doi: 10.21037/jgo-23-842